JOURNAL OF SPACECRAFT AND ROCKETS
Vol. 33, No. 6, November–December 1996

# Roll Torques Produced by Fixed-Nozzle Solid Rocket Motors

R. N. Knauber*
*Lockheed Martin Vought Systems, Dallas, Texas 75265-0003*

**Information about roll torques generated by solid rocket motors is needed for vehicle design to assess the impact on control requirements, flight dynamics, and accuracy. Several causes of roll torques, observed levels including statistical databases for several motors, a simple empirical approach for estimating magnitudes for conceptual and preliminary design, and a guide for steps in development and testing of solid rocket motors to measure roll torques are presented. Most of the data has been accumulated from exoatmospheric flight of the NASA solid controlled orbital and utility test vehicle (SCOUT) launch vehicle. Other ground test and flight data references are cited. Roll torques generated by internal vortex flow and nozzle ablation are the two most prominent sources. Transient torques having peak magnitudes as high as 163 N-m (120 ft-lbf) have been observed in exoatmospheric flights. There is no known method of predicting solid rocket motor generated roll torques of these types. Special ground and flight testing is required to accurately determine the magnitude for a specific motor design. Historical data indicate that smooth bore motors produce smaller roll torques than star grain or finned type grain motors.**

## Nomenclature

$D$ = motor diameter, m
$I_T$ = rocket motor total impulse, N-s
$I_x$ = roll mass moment of inertia, kg-m$^2$
$K_{JD}$ = roll jet damping efficiency factor
$K_{nf}$ = nondimensional peak roll torque factor
$K'_{nf}$ = nondimensional roll angular impulse factor
$L$ = roll torque, N-m
$\dot{m}$ = mass flow rate, kg/s
$p$ = roll rate, rad/s
$R$ = radius, m
$T$ = rocket motor thrust, N
$\Delta$ = incremental value

*Subscripts*

exit = rocket nozzle exit
max = maximum value

## Introduction

THE design of vehicles employing solid rocket motors requires assessment of the maximum roll torques, roll angular impulse, and time histories of roll torques to define control system requirements. These data are also needed to determine roll rate time histories of uncontrolled or passively spin stabilized vehicles.

Some solid rocket motors have been observed to produce significant levels of roll torque. Lack of knowledge of solid rocket motor roll torque generation has led to the failure of several launch vehicles. The Little Joe vehicle used to test the Mercury capsule more than 30 years ago inadvertently spun up at launch as a result of roll torques generated by the solid rocket booster. Roll torques generated by the third-stage rocket motor of the NASA solid controlled orbital and utility test vehicle (SCOUT) launch vehicle overpowered the control system on the first launch in 1960.[1]

There is no textbook or well-documented literature covering this subject. There is no widespread knowledge and understanding of the subject in technical circles either in propulsion houses or vehicle systems companies. The design engineer is left with a void of information. This paper provides data and an estimation procedure for flight dynamics or control engineers to evaluate the significance of this source of disturbance for new vehicle designs. A brief set of guidelines for development testing of motors for roll torques is also presented.

The author has observed vehicle behavior, extracted roll torques from flight data, planned and analyzed special ground tests of new motor designs, and applied this experience and data in vehicle design for several launch vehicles. Much of this experience was obtained with the NASA SCOUT, which used four solid rocket stages, all having fixed nozzles. SCOUT has used at least 13 different solid rocket motor designs with several modifications to some. The SCOUT database provided most of the statistical database used in this paper and in the empirical estimation. The empirical approach for conceptual design of roll control requirements has been used recently to support control system and accuracy studies for several multistage booster systems.

## Observation on Sources of Roll Torques

Solid rocket motors are designed and manufactured to be axially symmetric, well balanced, and devoid of features that would provide sources of large thrust misalignments, side forces, and roll torques. Yet motors do produce these disturbances. A fairly common misunderstanding is that the only way the solid rocket motor can produce roll torques is a coupling of the thrust misalignment vector with a radial center of mass offset. It is the author's experience with launch vehicles that this is a relatively small term compared with torques generated directly by the gas dynamics of some solid rocket motors. Not all motor designs produce measureable roll torques. Some produce well-defined characteristics; some produce very erratic torques.

In the early 1960s, there were several *AIAA Journal* articles on solid rocket motor roll torque generation.[2,3] Some associate high roll torques with acoustic instability.[2] Some motors have produced roll torques of several hundred newton-meters. Flight data for several variations of the smooth bore Star 37 used on the Burner II Program[4] are in the literature. Roll torque transients of 121 N-m (90 ft-lbf) were observed on Poseidon second-stage motors.[5] The latter had a 12 finned conocyl grain. SCOUT flight data indicated roll torques as high as 163 N-m (120 ft-lbf).[1,6–8] Static firing test data for the air-launched antisatellite (AL-ASAT) upper stage (Thiokol Star 20B) motor[9] and for the SCOUT Antares III (Thiokol Star 31) motor[10] indicated roll torques less than 6 N-m. Summary information is given in this paper.

Of all the information retrieved from the references and from experience, the author has identified four basic sources of solid rocket generated roll torques. For purposes of this paper roll torque will be identified as types I–IV.

Type I is large chamber vortex generation usually accompanied by some significant level of acoustic phenomena. When these large chamber vortices occur, the roll torque generated can be quite large.

Presented as Paper 95-2874 at the AIAA/ASME/SAE/ASEE 31st Joint Propulsion Conference, San Diego, CA, July 10–12, 1995; received Aug. 23, 1995; revision received June 21, 1996; accepted for publication July 9, 1996. Copyright © 1996 by R. N. Knauber. Published by the American Institute of Aeronautics and Astronautics, Inc., with permission.

*Consulting Engineer, Flight Dynamics and Aerodynamics, Mail Stop EM-55. Senior Member AIAA.

Type II is short-lived transients that occur at specific times in the burn-back profile. Torques can be either unidirectional or can exhibit an almost instantaneous reversal in sense.

Type III is small unidirectional quasisteady roll torques caused by ablative patterns in nozzles. Similar phenomena have been observed on early ablating re-entry vehicles.

Type IV is conservation of angular momenta of spinning rockets, observed roll jet damping as a result of changing angular velocity of chamber gases interacting with the walls of the converging-diverging nozzle walls.

Motors having a smooth bore grain geometry with or without radial slots appear to generate little or no roll torque of types I and II. Most motors having star grains, longitudinal slots, or finned grain geometry appear to generate type I or II transients.

## Case Histories and Data

Some of the motor designs flown on SCOUT, AL-ASAT, and other programs are shown in Table 1. The case histories are presented by type.

### Type I

The first launch of the NASA SCOUT launch vehicle in 1960 used an Allegheny Ballistics Laboratory (ABL) X-254 Antares I third-stage rocket motor; see Fig. 1. This motor was an acoustically unstable burner that included an internally mounted detuning paddle. It had a center perforated grain geometry with five longitudinal slots. The roll torque generated late in the burn was accompanied by high levels of acoustically induced vibration. The level was sufficient to overpower the small reaction control system, which resulted in loss of the guidance roll reference.[1] Subsequent ground testing, with a specially designed test stand, reproduced the observed behavior on the ground. The control system was redesigned, and this motor was flown on seven more vehicles.

Relationship of roll torque generation to acoustic instabilities was reported on other motors in the past.[2,3,5] The author has not seen evidence of any significant roll torques of types I or II on smooth bore motors (no longitudinal slots or fins). The directed flow out of a slot coupled with very small dissymmetry could be the source of large internal vortex generation.

### Type II

There are several motor designs that have produced repeatable roll torque transients. The Thiokol Castor I motor is one of these. This fixed-nozzle steel case motor was flown on the first 39 SCOUT flights as a second stage. Ignition occurred above 43-km (140,000-ft) altitude where aerodynamic disturbances are insignificant. On all flights this motor produced a roll left torque that reached a maximum value about 0.4 s after ignition (Fig. 2). After reaching this peak value, the magnitude slowly decayed to an insignificant level 8 s after ignition. The magnitude varied from flight to flight. The peak value observed was 163 N-m (120 ft-lbf) out of 21 flights. This motor had a five point star grain geometry over most of the bore length. The peak value of torque exceeded the roll control system capability, but the duration was short enough to prevent loss of control.

The SCOUT second stage later used the Thiokol Castor II, which had the same external envelope but more total impulse. The grain geometry was changed to a center perforation with two radial slots (Fig. 3). Maximum roll torques observed in flight are an order of magnitude less than the Castor I. No torques above 7 N-m have been observed.

The Hercules X-259 Antares II motor used as a third stage on SCOUT for nearly two decades also produced a type II roll torque transient. On almost every flight the transient roll torque would peak about 3–6 s into the burn period (Fig. 4). The buildup to the peak value would often be exponential and would sometimes reverse polarity within 0.1 s and then rapidly decay in magnitude. This motor had a center perforated grain with an X-slot in the aft half of the propellant. This motor was flown on 49 flights with no control problems.

A modification to the X-259 motor was made to increase performance. It was designated HP-X-259 Antares IIB for SCOUT usage. The nozzle was replaced with one that had a smaller throat area, which increased the chamber pressure by 70% and reduced the burn time. There was no change to the propellant or grain geometry.

**Table 1 Solid rocket motor roll torque**

| Motor description | Diam., mm | Thrust, kN | Impulse, kN-s | Torque, N-m | Ang. imp., N-m-s | Type | Sample size | $k_{nf}\times$ 1000 | $k'_{nf}\times$ 1000 | Grain shape |
|---|---|---|---|---|---|---|---|---|---|---|
| Hercules ABL X-254 | 762 | 62.3 | 2380 | 36.59 | 135.50 | I | 4 | 0.7708 | 0.0747 | Five slot |
| Hercules X-259 | 762 | 106.7 | 3210 | 12.20 | 40.65 | II | 49 | 0.1501 | 0.0166 | X-slots |
| Hercules HP-X-259 | 762 | 146.8 | 3320 | 23.04 | 40.65 | II | 3 | 0.2060 | 0.0161 | X-slots |
| Thiokol Castor I | 787 | 290.0 | 8720 | 169.38 | 304.88 | II | 21 | 0.7421 | 0.0444 | Five point star |
| Posiedon second stage | 2108 | 1335.0 | 93400 | 121.95 | 487.80 | II | 9 | 0.0433 | 0.0025 | 12 fin |
| Thiokol Star 31 | 762 | 83.0 | 3710 | 4.74 | 94.85 | III | 12 | 0.0749 | 0.0336 | Smooth |
| Thiokol Castor II | 787 | 267.0 | 10230 | 6.78 | 81.30 | III | 78 | 0.0323 | 0.0101 | Smooth |
| Star 37 early nozzle | 940 | 47.0 | 1870 | 2.71 | 29.81 | III | 8 | 0.0613 | 0.0170 | Eight point star |
| Star 37 rosette nozzle | 940 | 68.0 | 2910 | 4.20 | 90.79 | III | 13 | 0.0657 | 0.0332 | Eight point star |
| UTC FW-4S spin | 508 | 28.9 | 774 | 0.27 | 2.71 | IV | 12 | 0.0184 | 0.0069 | Smooth |
| Thiokol Star 20A spin | 508 | 29.4 | 778 | 0.27 | 2.71 | IV | 20 | 0.0181 | 0.0069 | Smooth |
| Thiokol Star 20B AL-ASAT | 508 | 29.4 | 778 | nil | nil | —— | 3 | nil | nil | Smooth |

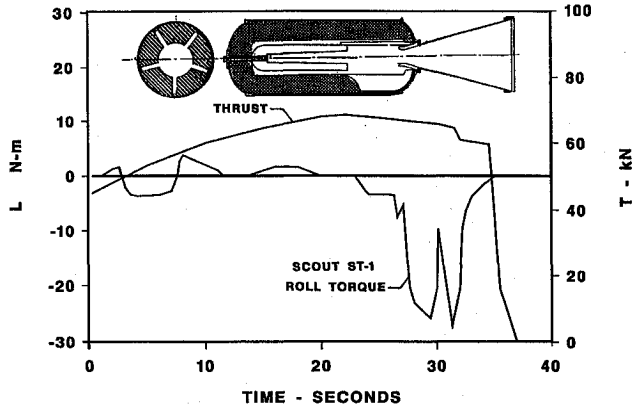


Fig. 1 ABL X-254 Antares I roll torque.

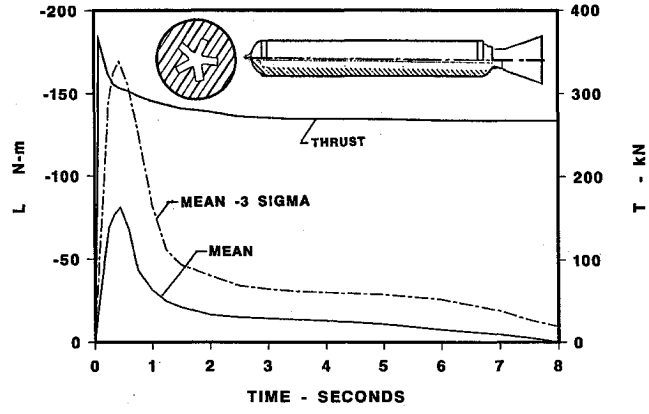


Fig. 2 Castor I roll torque transient.

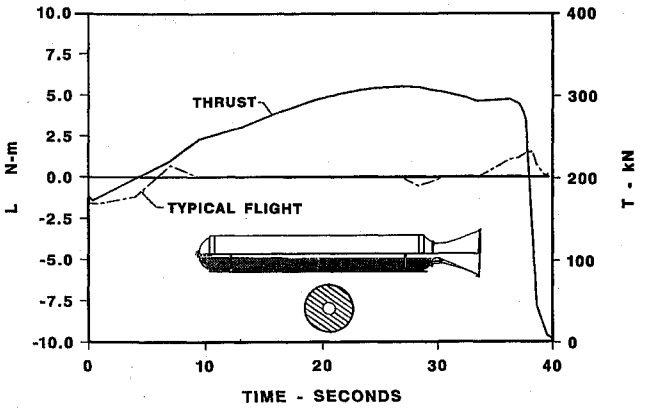


Fig. 3 Castor II roll torque.

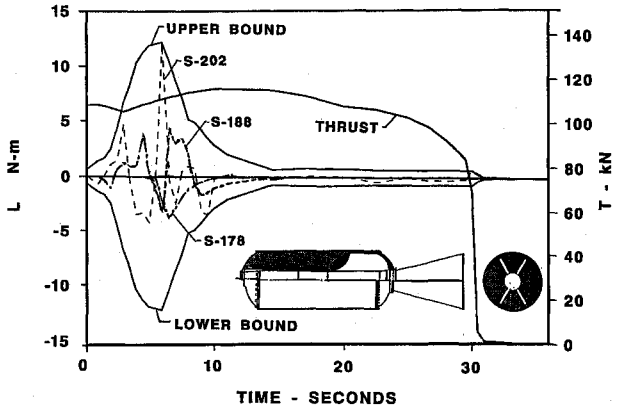


Fig. 4 X-259 Antares II roll torque.

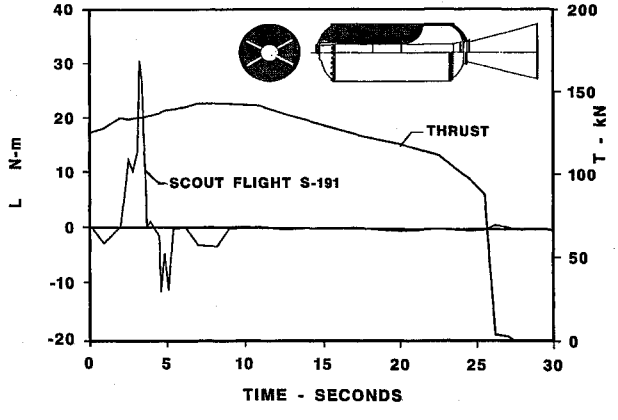


Fig. 5 HP-X-259 Antares IIB roll torque.

It was flown on only three SCOUT flights. The increased flow rate and reduced burn time altered the roll torque transient (Fig. 5). The transient occurred earlier (about the same place in the burn-back profile), and the magnitude was about twice as much as observed on the X-259 Antares IIA motor.

Transient roll torques, similar in trend to the X-259 motor, were reported on the Poseidon second-stage motor.[5] The rapid buildup and decay was sometimes accompanied by an instantaneous reversal in polarity. The magnitudes of torque were considerably larger, up to 122 N-m (90 ft-lbf). The motor size was also much larger. This motor had a center perforated grain with a 12 fin forward slot geometry.

**Type III**

The Thiokol Star 31 Antares III motor was flown on the last 13 flights of SCOUT. This motor has a center perforated bore with a single aft radial slot (see Fig. 6). There is no evidence of type I or II roll torques. However, this motor does produce a consistent low-level roll-right torque throughout the burn period.

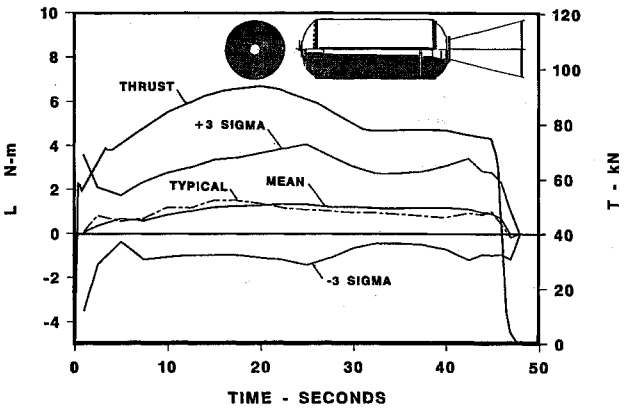


Fig. 6 Star 31 Antares III roll torque.

Review of pre- and postfiring nozzles indicates that the nozzle exit cone (tape wound rosette pattern) ablates to produce a slight pinwheel effect consistent with the roll right torque. A similar phenomenon occurred on some early ablative re-entry vehicles, which subsequently were redesigned to change the tape lay-up pattern. The Star 31 torques did not cause any problems to the SCOUT third-stage roll control system.

A similar unidirectional roll torque of the type III was reported on the Star 37 motors used in the Burner II Program.[4] By changing the nozzle liner lay-up from a rosette pattern to a bulk lay-up, the roll torque was reduced in magnitude and became random in polarity.

**Type IV**

Conservation of angular momentum of spinning rockets results in "jet damping" terms through the reaction of gases between the burning surface and their path to the nozzle exit. As the gas enters the nozzle to a smaller radius, conservation of angular momentum dictates that the gas vortex must spin faster than the rest of the body. As it expands out the diverging exit cone, the average gas angular velocity decreases relative to the spin rate of the body. The changing angular velocity of the gases along the exit path interact with the uniform angular velocity of the rocket grain and nozzle to impart some exchange of angular momentum.

An oversimplification would be to treat the exiting gas as a pseudorigid body that had a uniform angular rate at the nozzle exit. If the gas disk at the exit plane of the nozzle rotated at the same angular velocity as the nozzle lip, there would be a relatively large jet damping term. In this exaggerated case the jet damping torque would be

$$\Delta L = -\left[\dot{I}_x + \frac{\dot{m}R_{\text{exit}}^2}{2}\right]p \tag{1}$$

In Eq. (1), the rate of change of roll inertia is a negative number, and the mass flow rate is a positive number.

Full spin accommodation of the exiting gas with the nozzle is not realized. Through skin-friction drag, the swirling gases impart a local roll torque to the nozzle. Computation of the flow and roll torque reaction on the nozzle walls is a rather complex fluid dynamic problem to solve to any degree of accuracy. Empirical test data are helpful for estimating the degree of exchange of angular momentum. An efficiency factor is added to the simple pseudorigid model to fit experimental flight data; i.e.,

$$\Delta L \cong -K_{JD}\left[\dot{I}_x + \frac{\dot{m}R_{\text{exit}}^2}{2}\right]p \tag{2}$$

The last 66 SCOUT vehicles used either the United Technologies Corporation (UTC) FW-4S or the Thiokol Star 20A Altair IIIA, both smooth bore motors not exhibiting any types I, II, or III roll torques symptoms. The only noticeable change in spin rate is from the jet damping and other conservation of angular momenta effects. The spin rate and jet damping torque are shown in Fig. 7. The empirically derived jet damping efficiency factor is 0.067.

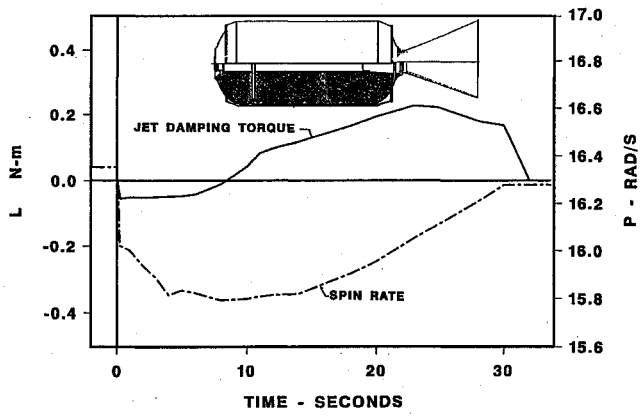


**Fig. 7 SCOUT fourth-stage spin rate: Star 20A.**

Another conservation of angular momenta effect has been observed on the SCOUT fourth-stage motor. The motor is separated at orbital altitude while spinning and is ignited several seconds later. When the motor ignites, the pressure buildup increases the diameter of the motor case and propellant by approximately 2.5 mm (0.1 in.). This causes a sudden increase in roll moment of inertia. Conservation of angular momentum causes the sudden decrease in spin rate at ignition (Fig. 7).

The apparent torques from these dynamic effects are small. The maximum jet damping equivalent torque is less than 0.3 N-m.

## Empirical Roll Torque Prediction Method

An empirical method of estimating maximum roll torques produced by solid rocket motors is needed for conceptual and preliminary vehicle design. A set of nondimensional factors $K_{nf}$ and $K'_{nf}$ are used to provide a conservative estimate of the peak roll torque and angular impulse imparted during the burn phase. These factors are nondimensionalized by motor diameter, thrust level, and total impulse. Table 1 provides a summary of types I, II, and III roll torques and roll torque impulses for many different motor designs. The dimensions, thrust, impulse, grain geometry, number or samples in the database, maximum roll torque, and maximum angular impulse are summarized.

The peak roll torque is nondimensionalized by the thrust at the peak and the motor diameter; i.e.,

$$K_{nf} = \frac{L_{\max}}{T_{\max} D} \tag{3}$$

The angular impulse produced by the torque is similarly nondimensionalized; i.e.,

$$K'_{nf} = \frac{\int L\,dt}{I_T D} \tag{4}$$

Roll torque and angular impulse for an untested design demands conservative estimates. Assuming that the new design has no significant acoustically unstable characteristics, the type I factor could be eliminated. The method uses the following steps and $K_{nf}$ and $K'_{nf}$ factors from Table 1.

1) If the motor has long longitudinal slots, include a conservative estimate of the type II factor; as an example, for Castor I $K_{nf} = 0.000744$.

2) If the nozzle exit cone is to be a tape lay-up type, include the type III factor from the Star 31, $K_{nf} = 0.000075$.

3) If the motor is spinning, include the jet damping term, Eq. (2), with an efficiency factor, $K_{JD} = 0.07$.

4) Since the types II and III effects are independent sources and represent several standard deviations, they should first be statistically combined. As shown in the actual databases, there may be a nonzero mean value either roll right or roll left. A conservative approach would be to add the two $K_{nf}$ factors arithmetically before applying to the thrust time history.

For example, if the Castor I data were used to estimate the type II transient torque potential of the X-259, the following data would be used:

$$\text{Castor I, } K_{nf} = 0.000742$$

$$\text{X-259, } T_{\max} = 106{,}700 \text{ N; } D = 0.762 \text{ m}$$

$$L_{\max} = (0.000742)(106{,}700)(0.762) = 60.6 \text{ N-m}$$

The peak value observed out of 49 flights was about 12 N-m. The estimate based on the three sigma value of the Castor I is very conservative. The highly transient peak torques, types I and II, are not readily predictable. Unfortunately, types I and II sources can produce much larger roll torques than the other sources. Motors that tend toward acoustic instability can produce very large type I torque. Type III disturbances are more predictable but of lesser significance. Therefore, conservatism should be used in the early design phases. There is an order of magnitude variation in the nondimensionalized peak torque parameters of the motors in the database (Table 1).

## Testing

If the empirical estimates of roll torques are large enough to be a potential problem to the vehicle design, plans should be made to obtain test data from static firing and flight test. The actual forces produced by the roll torques on a six-component test stand are several orders of magnitude lower than the primary thrust and side forces. For example, the relatively high roll torque produced by the X-254 is less than 37 N-m. The thrust forces are 63 kN, and the weight of the motor and holding cage is in excess of 11 kN. It is obvious that accurate measurement of the roll torques requires tight tolerances, precision instrumentation, precise stand and motor alignments, and sophisticated data reduction techniques. The accuracy and precision of the test setup, calibration, and data reduction process are pushing the state of the art in current solid rocket motor test facilities to measure roll torques as low as the Star 31 (4 N-m maximum with 80-kN thrust).

The author has seen two techniques that worked within reasonable bounds for the larger roll torques. A special test stand was designed, built, and used by NASA Langley Research Center to test the X-254 in 1960. The Langley stand used hydraulically suspended roll supports (fluid bearings both radial and axial), with a shaker to dither the motor in roll. Roll torques were measured with a load cell connection that restrained the cage from rolling. Although this has proven to be a good stand for measuring roll torques, the author is unaware of the use of similar designs being used in recent years.

Another roll torque test measurement technique was used for the Star 20B[9] and the Star 31[10] motors. Qualification altitude tests were performed at the U.S. Air Force Arnold Engineering Development Center (AEDC) in the T-3 spin test facility. Roll torques were extracted with ±7 N-m accuracy using existing hardware and instrumentation. By spinning the motors at a slow spin rate (30 rpm), side forces could be extracted more accurately than in a fixed six-component stand. Roll torques were measured by monitoring the spin rate time history, roll drive system electrical or hydraulic parameters, characterizing the thrust bearing friction, and using special data reduction techniques. Actual roll torque obtained from flight testing was much less than the accuracy of the ground test data. The unidirectional 1–4 N-m roll torque that the Star 31 produced on the SCOUT flights was indistinguishable from the AEDC thrust bearing friction uncertainty. Ground test data provide a conservative estimate of roll torques if a sufficient sample size is tested.

## Conclusions

Fixed-nozzle solid propellant rocket motors can produce roll torques significant to the flight dynamics and control engineer. Characterization and prediction of roll torques are not an exact science. The simple empirical approach using the nondimensional $K_{nf}$ and $K'_{nf}$ factors should provide conservative estimates for conceptual and preliminary designs. If these estimates are significant for the application, further characterization by ground static firing and flight testing is recommended.

An observation that may be of importance to future designers and analysts can be summarized as follows: smooth bore motors = small torques and longitudinal slots = large torques!

## References

[1]Mayhue, R. J., "NASA SCOUT ST-1 Flight Test Report," NASA TN D-1240, June 1962.

[2]Flandro, G. A., "Roll Torque and Normal Force Generation in Acoustically Unstable Rocket Motors," *AIAA Journal*, Vol. 2, No. 7, 1964, pp. 1303–1306.

[3]Swithenbank, J., and Sotter, G., "Vortex Generation in Solid Propellant Rockets," *AIAA Journal*, Vol. 2, No. 7, 1964, pp. 1297–1302.

[4]Dionne, E. R., Kossman, W. J., and Klemetson, R. W., "Characterization of the Non-Axial Thrust Generated by Large Solid Popellant Rocket Motors in Three Axis Stabilized Vehicles," AIAA Paper 78-1076, July 1978.

[5]Pendleton, L. R., "Sinusoidal Vibration of Poseidon Solid Propellant Motors," *The Shock and Vibration Bulletin*, Pt. 3, Bulletin 42, Shock and Vibration Information Center, Naval Research Lab., Office of the Director of Defense Research and Engineering, Washington, DC, Jan. 1972, pp. 89–98.

[6]Knauber, R. N., "SCOUT Second Stage Roll Transient Anomaly Investigation," Lockheed Martin Vought Systems, Rept. 23.255, Dallas, TX, Jan. 1966.

[7]Knauber, R. N., "SCOUT Altair III (Thiokol Star 20A) Roll Torque Data Flight Experience," Lockheed Martin Vought Systems, Rept. 211-06-AI-30029, Dallas, TX, Jan. 1983.

[8]Teague, H. D., and Black, C. E., "SCOUT Flight Data Historical Summary—Volumes I and II," Lockheed Martin Vought Systems, Rept. 3-34100/9R-12, Revision C, Dallas, TX, June 1977.

[9]Knauber, R. N., "ASAT Upper Stage Motor AEDC Side Force and Roll Torque Test Data," Lockheed Martin Vought Systems, Rept. 211-07-AG-30202, Dallas, TX, June 1983.

[10]Knauber, R. N., "SCOUT Antares III Integration—Stability and Control," Lockheed Martin Vought Systems, Rept. 23-DIR-2151, Dallas, TX, Aug. 1979.

J. C. Adams
*Associate Editor*

**Humans in Spaceflight**

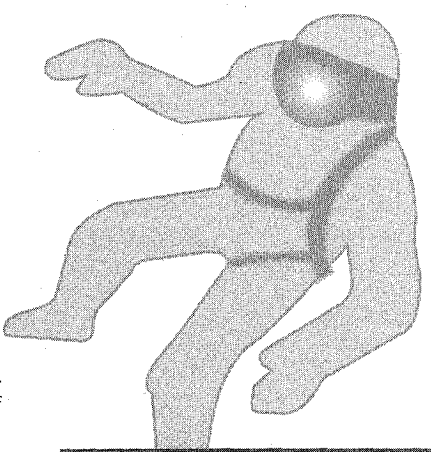

Volume III in the "Space Biology and Medicine" series, Humans in Spaceflight, edited by Carolyn Leach Huntoon, Ph.D., addresses the major issues concerning humans in space such as metabolism, the immune system, neurosensory and sensory motor functions, gravitational biology, radiation, pharmacokinetics, and much more. It is composed of two parts: "Effects of Microgravity" and "Effects of Other Spaceflight Factors." As in the previous two volumes, the contributing authors are experts in their respective fields.

Life Support and Habitability
1994 423 pp Cloth
ISBN 1-56347-082-9
AIAA Members $69.95
List Price $99.95
Order #: 82-9(945)

Space and Its Exploration
1993 338 pp Cloth
ISBN 1-56347-061-6
AIAA Members $69.95
List Price $99.95
Order #: 61-6(945)

FALL 1996 Cloth
ISBN 1-56347-180-9
AIAA Members $99.95
List Price $129.95
Order #: 80-9(945)

**Place your order today!**
**Call 800/682-AIAA**

AIAA
American Institute of Aeronautics and Astronautics

Publications Customer Service, 9 Jay Gould Ct., P.O. Box 753, Waldorf, MD 20604 FAX 301/843-0159 Phone 1-800/682-2422 9 a.m. - 5 p.m. Eastern